Journal of Magnetism and Magnetic Materials 529 (2021) 167902

Contents lists available at ScienceDirect

Journal of Magnetism and Magnetic Materials

journal homepage: www.elsevier.com/locate/jmmm

Research articles

Interaction between magnetic molecules and two ferromagnetic electrodes of a magnetic tunnel junction (MTJ)

Marzieh Savadkoohi, Bishnu R. Dahal, Andrew Grizzle, Christopher D'Angelo, Pawan Tyagi *

Center for Nanotechnology Research and Education, Mechanical Engineering, University of the District of Columbia, Washington, DC 20008, USA

ARTICLE INFO

Keywords:
MTJ
SMM
Spintronics
Ferromagnetism
Tunnel barrier
Exchange coupling

ABSTRACT

This paper focuses on Monte Carlo Simulations (MCS) to investigate the effects of variations in molecular exchange coupling strengths and nature between the magnetic molecules and ferromagnetic electrodes in cross-junction-shaped magnetic tunnel junction (MTJ) based molecular spintronics devices (MTJMSD). To encompass a wide range of futuristic molecular spintronics devices, we systematically studied the effect of a magnetic molecule analog coupling with two ferromagnetic electrodes. We studied three cases when molecules established: (i) Ferromagnetic couplings with two ferromagnetic electrodes, (ii) Antiferromagnetic couplings with two electrodes, and (iii) Ferromagnetic coupling with one electrode and antiferromagnetic coupling with another electrode. We varied the strength and nature of exchange coupling to study the temporal and spatial propagation of molecular coupling impact on two ferromagnetic electrodes. Our results showed that in the cases when molecular coupling strength was ~ 10% of the ferromagnetic electrode's Curie temperature, then 16 molecular analogs could influence the magnetic properties of 2,500 atoms above room temperature. This theoretical study is directly in agreement with the experimental observation of ~ 10,000 Single Molecular Magnet (SMM) channels controlling the magnetic and transport properties of microscopic cross-junction-shaped MTJ testbed above room temperature.

1. Introduction

Molecular spintronics devices (MSDs) are a potential candidate for futuristic advanced memory devices and computational technologies, including quantum computation [1–3]. Utilizing the spin property of electrons by placing molecular bridges between metal leads open a wide range of opportunities to observe and discover novel phenomena and device mechanisms. Molecules are also endowed with low spin scattering advantages. Molecules can exhibit low hyperfine splitting and Zeeman effects [4–7]. Molecular spintronics devices can consume significantly less power and lead to the next generation of memory and computational devices [8].

In previous studies, molecules were bonded to two conducting electrodes by several methods [9,10]. These methods imposed challenges in including a wide range of metal electrodes, including ferromagnetic electrodes needed for MSDs fabrication. Researchers have employed a break junction or nanogap junction approach to connect ferromagnetic electrodes to the molecules [11]. Few studies have focused on sandwiching molecules between ferromagnetic electrodes [12]. However, a defect-free monolayer formation for molecular device realization is strongly dependent on metal substrate type. Several review papers have extensively discussed the limitations of the conventional molecular device fabrication approaches [13]. Magnetic tunnel junction-based molecular spintronic devices (MTJMSDs) were designed and tested to address significant MSD fabrication challenges [14].

MTJMSDs have a multilayer-shaped structure in which two layers of ferromagnetic (FM) electrodes are separated by a ~ 2 nm thick insulator, a.k.a tunneling barrier (Fig. 1a) [14,15]. Magnetic molecules are covalently bonded to two FM electrodes across the tunneling barrier (Fig. 1b). Depending on the nature of ferromagnetic material, the functional anchoring group, tether molecules, and the core of the molecule, one can observe a wide range of molecular coupling strengths and nature. For instance, if a paramagnetic molecule is connected to a ferromagnetic nickel layer via anchoring functional groups, such as sulfur, oxygen, –NH, –CN, etc., MTJMSD will produce different types of the molecule -FM coupling. On the other hand, if tether molecules are alkane (insulator), alkene (semiconductor), alkyne (conducting), the strength of molecule-FM electrode coupling is expected to be quite

* Corresponding author.
E-mail address: ptyagi@udc.edu (P. Tyagi).

https://doi.org/10.1016/j.jmmm.2021.167902
Received 10 January 2021; Received in revised form 12 February 2021; Accepted 1 March 2021
Available online 10 March 2021
0304-8853/Published by Elsevier B.V.

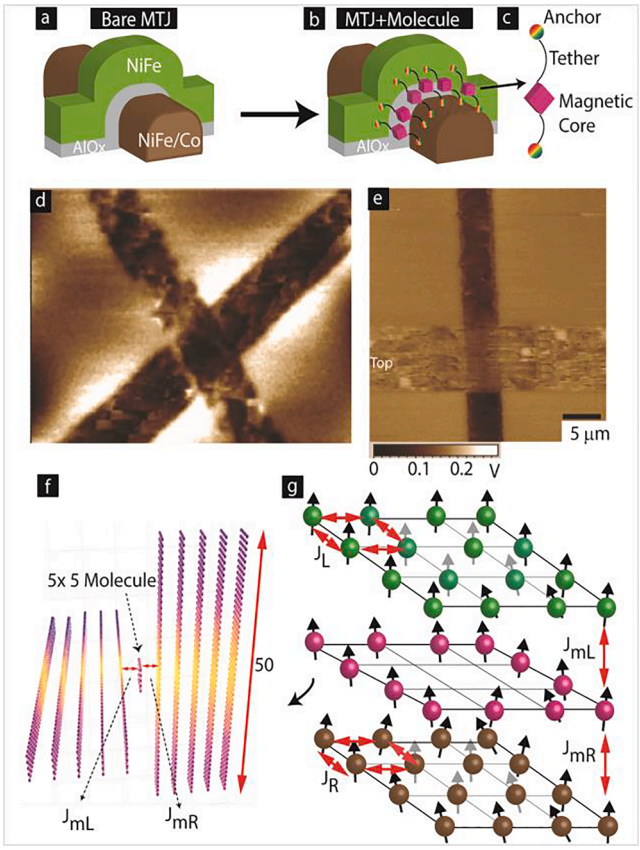

Fig. 1. MTJMSD 3D-architecture (a) before and (b) after magnetic molecules treatment (c) magnetic molecule composition (d) bare MTJ's MFM image (e) MTJMSD MFM image after making molecular attachment (f) 3D MTJMSD Ising model analogues to MTJMSD in panel (b). (g) 3D Ising model describing inter- and intra-atomic Heisenberg exchange coupling energies between FM electrodes and magnetic molecules.

different [16]. We have experimentally observed unprecedented paramagnetic molecule induced exchange coupling impacting the microscopic ferromagnetic electrodes with the MTJMSD device approach [15,17–20]. For example, Fig. 1d shows a MTJ testbed before hosting paramagnetic molecular channels in the manner shown in Fig. 1b. After establishing molecular spin channel, MTJ started exhibiting remarkably different magnetic contrast in the Magnetic Force Microscopy study (Fig. 1e). More details about the other supporting experiments and MFM experiments are published elsewhere [15,17–20].

It is challenging to experimentally study all possible cases of MTJMSDs that may arise when a magnetic molecule interacts with the two FM electrodes. This paper utilizes Monte Carlo simulations (MCS) [21,22] to investigate the effect of nature and strength of magnetic coupling that a magnetic molecule may encounter while simultaneously bonded to two FM electrodes of a MTJ. We represented the magnetic molecule coupling with two FM electrodes by Heisenberg exchange parameters. By changing the exchange coupling parameters over a wide range, we attempted to encompass a large variety of possible MSDs that may be experimentally realized.

2. Methodology

Monte Carlo Simulation (MCS) was used to investigate the magnetic properties of cross-junction-shaped MTJMSDs. Cross junction shape MTJMSD possesses elongated FM electrodes enabling the outer-world connection with the molecular junction site. MTJMSD model simulated in this study was inspired by our prior continuous spin MCS study explaining the experimental results on pillar shaped MTJMSD, i.e., without any elongated FM electrodes [15]. In prior work, we were unable to investigate the impact of large FM electrodes on the magnetic molecule induced properties of MTJMSD. In previous research, organometallic molecular clusters (OMC) were attached to two FM electrodes (Fig. 1(a–c)) and made antiferromagnetic coupling with one FM electrode and ferromagnetic coupling with the other FM electrode [15,17].

The magnetic interaction between two FM electrodes is possible via molecular channels. To avoid computational complications associated with complex and transition metal-based molecules, we have represented molecule with a simple atomic shaped analog [15]; hereafter referred to as molecule or molecular analog, in this manuscript. We represented molecule-FM electrode coupling as the Heisenberg exchange coupling. For the practical temperature range, we kept thermal energy (kT) to be 0.1. $kT = 0.1$ will be equivalent to 50–90°C, assuming FM electrode Curie temperature in 500 *to* 900 $^{\circ}C$ temperature range [23]. The size of the MTJMSD Ising model in our MCS study is H × W × L (=11 × 50 × 50), where H is the atomic height, W is the atomic width, and L is the atomic length. The molecular plane is a 5 × 5 atomic square with an empty interior inserted along the H dimension of the MTJ. The molecular plane is located at the cross-junction of two five monolayers thick and 50 atom long FM electrodes (Fig. 1f). To achieving the energy equilibrium state, the system's energy was minimized according to the following equation:

$$E = -J_L\left(\sum_{i\in L}\vec{S}_i\vec{S}_{i+1}\right) - J_R\left(\sum_{i\in R}\vec{S}_i\vec{S}_{i+1}\right) - J_{mL}\left(\sum_{i\in L, i+1\in mol}\vec{S}_i\vec{S}_{i+1}\right) - J_{mR}\left(\sum_{i-1\in mol, i\in R}\vec{S}_{i-1}\vec{S}_i\right) \quad (1)$$

Where S represents the spin of individual atoms of FM electrodes and molecule in the form of a unit magnitude 3D vectors. Fig. 1g represents the parameters associated with FM electrodes and FM-molecule interactions. J_L, and J_R, are the Heisenberg exchange coupling strengths for the left and right FM electrodes, respectively. J_{mL} and J_{mR} are the Heisenberg exchange coupling strengths between the left FM electrode and molecules and right FM electrodes and molecules, respectively (Fig. 1g). To simulate a wide range of weak to strong ferromagnetic and antiferromagnetic coupling possibilities between FM electrodes and molecule, we varied the nature and strengths of J_{mL} and J_{mR}. Here, we supposed that inter-FM electrode exchange coupling is zero, and thus there is no leakage or conduction between ferromagnetic electrodes via tunneling barrier. The topic of direct coupling between ferromagnetic electrode is beyond the scope of the current paper because of two

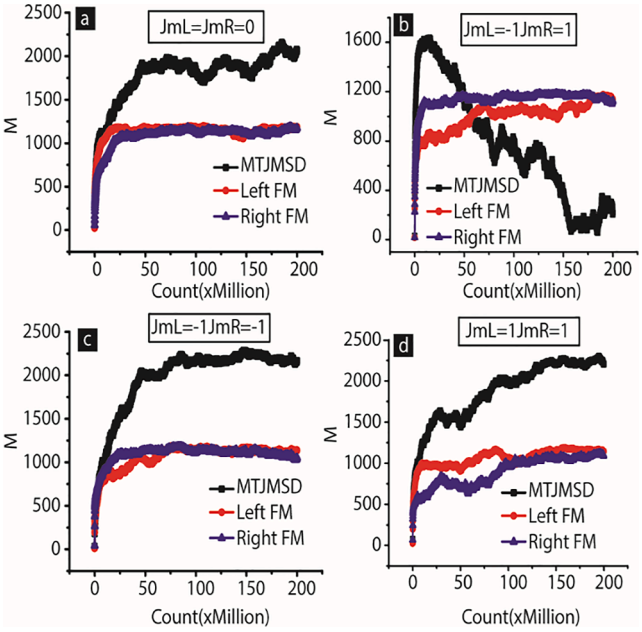

Fig. 2. Magnetic moment *(M)* vs. simulation count of the MTJMSD, left ferromagnet (left-FM), right ferromagnet (right-FM) for the cases of (a) *JmL*=*JmR*=0, (b) *JmL*=−*1, JmR*=1, (c) *JmL*=−*1, JmR*=−1, and (d) *JmL*=*JmR*=1.

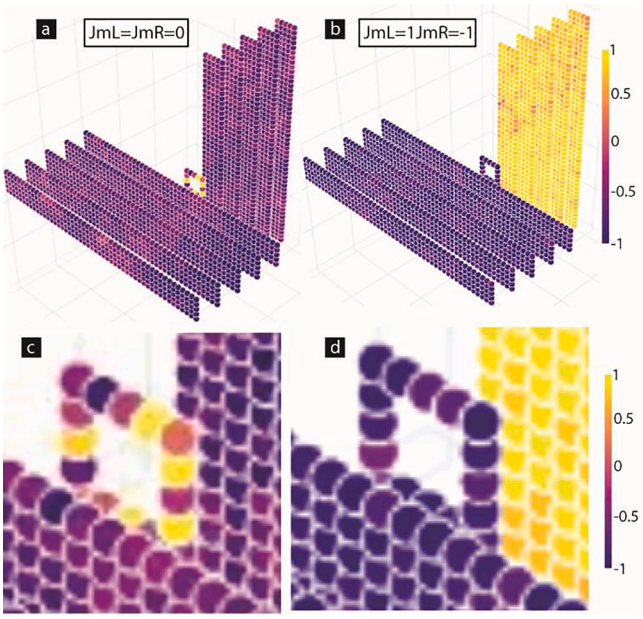

Fig. 3. Simulated 3D Plots of MTJMSD for (a) *JmL*=*JmR*=0 and (b) *JmL*=*1, JmR*=−1. Magnified version of molecular spin orientation for (c) *JmL*=*JmR*=0 and (d) *JmL*=*1, JmR*=−1.

reasons: (a) this paper focuses on molecular coupling in the presence of an ideal physical gap in the junction area providing insignificant interaction, (b) if tunnel junction is defective there exist many possibilities of magnetic interaction via a physical gap (tunnel junction) and hence extensive discussions are required to cover the direct coupling impact on MTJMSD. The impact of direct interaction between two magnetic layers on MTJMSD is a comprehensive research topic. We have recently published preliminary Monte Carlo Simulations about the role of direct exchange coupling elsewhere [22]. Also, we supposed that both FM electrodes have initial parallel magnetization with respect to each other during the entire simulation. Initial spin state of molecules and right FM electrode and left FM electrode were fixed to be 1. During simulation, spins could rotate in spherical coordinates randomly. Equilibrium energy state is determined through the Metropolis algorithm and Markov process [15]. Each Monte Carlo simulation was run for 200 million iterations to achieve a stable low energy state. At the equilibrium state, the spin vectors settle in any direction due to a continuous model used in our MCS study. Sum of the magnetic moment of the left and right FM electrodes and molecules give the total device magnetic moment. We also investigated the spatial correlation between molecular spin and FM electrodes. In addition, we measured the molecular coupling impact on the spatial magnetic susceptibility.

3. Results and discussion

MTJMSD was found to settle in different current states with time [17,19]. Temporal evolution of MTJMSD's magnetic properties was studied for a variety of couplings strengths and nature between molecules and FM electrodes. We studied full range of JmL and JmR coupling values between −1 to 1 with step 0.2. This produced 121 datasets which contain variety of molecules-FM electrodes magnetic interactions. We represented the temporal evolution phase or time in MCS as the simulation count. MTJMSD and FM electrodes' magnetic moment were recorded during the MCS period, typically 200 million counts. Based on the Ising Model utilized in this study, left-FM and right- FM electrodes can attain the maximum magnetic moment of 1250 magnitude. The overall MTMSD magnetic moment can be nearly 2500. Fig. 2 represents the time-dependent evolution of the magnetic moment of the overall MTJMSD, left FM, and right FM electrodes. In the case of $JmL = JmR = 0$, MTJMSD's magnetic moment settled arbitrarily (Fig. 2a). However, the strong magnetic coupling between FM electrodes and molecules resulted in significant variation in MTJMSD magnetization. For the case of molecule induced strong antiferromagnetic coupling ($JmL = -1$ and $JmR = 1$), two FM electrodes evolved to be antiparallel to each other. For this case, the trend observed in Fig. 2b is consistent with the experimental observation of various magnetic and transport characteristics during the initial stage of MTJMSD formation [17,19]. For $JmL = -1$ and $JmR = 1$, it is remarkable that ~ 16 molecules are capable of forcing two large FM electrodes to be in the antiparallel state in which left-FM and right-FM electrodes cancel each other magnetic moment. In this state, MTJMSD's magnetic moment settled to close to zero and is believed to be the basis of the observed current suppression phenomenon [17]. We envision that based on molecule and FM electrode types, there is a possibility where a molecule can form either antiferromagnetic ($JmL = -1$ and $JmR = -1$) or ferromagnetic coupling ($JmL = 1$ and $JmR = 1$) with the two FM electrodes. We have simulated the time evolution of MTJMSD in other such possible scenarios. In the case of $JmL = -1$ and $JmR = -1$, the molecule aligned antiparallel with respect to two FM electrodes (Fig. 2c). Similarly, for $JmL = 1$ and $JmR = 1$, the molecule layer aligned parallel with respect to two electrodes (Fig. 2d). In both cases, two FM electrodes were forced to be parallel, and hence MTJMSD magnetic moment was governed by the addition of the moments of Left-FM and Right-FM. Consequently, strong couplings between 1250 atom FM electrodes through 16 magnetic molecules show the stable impact on overall device magnetization.

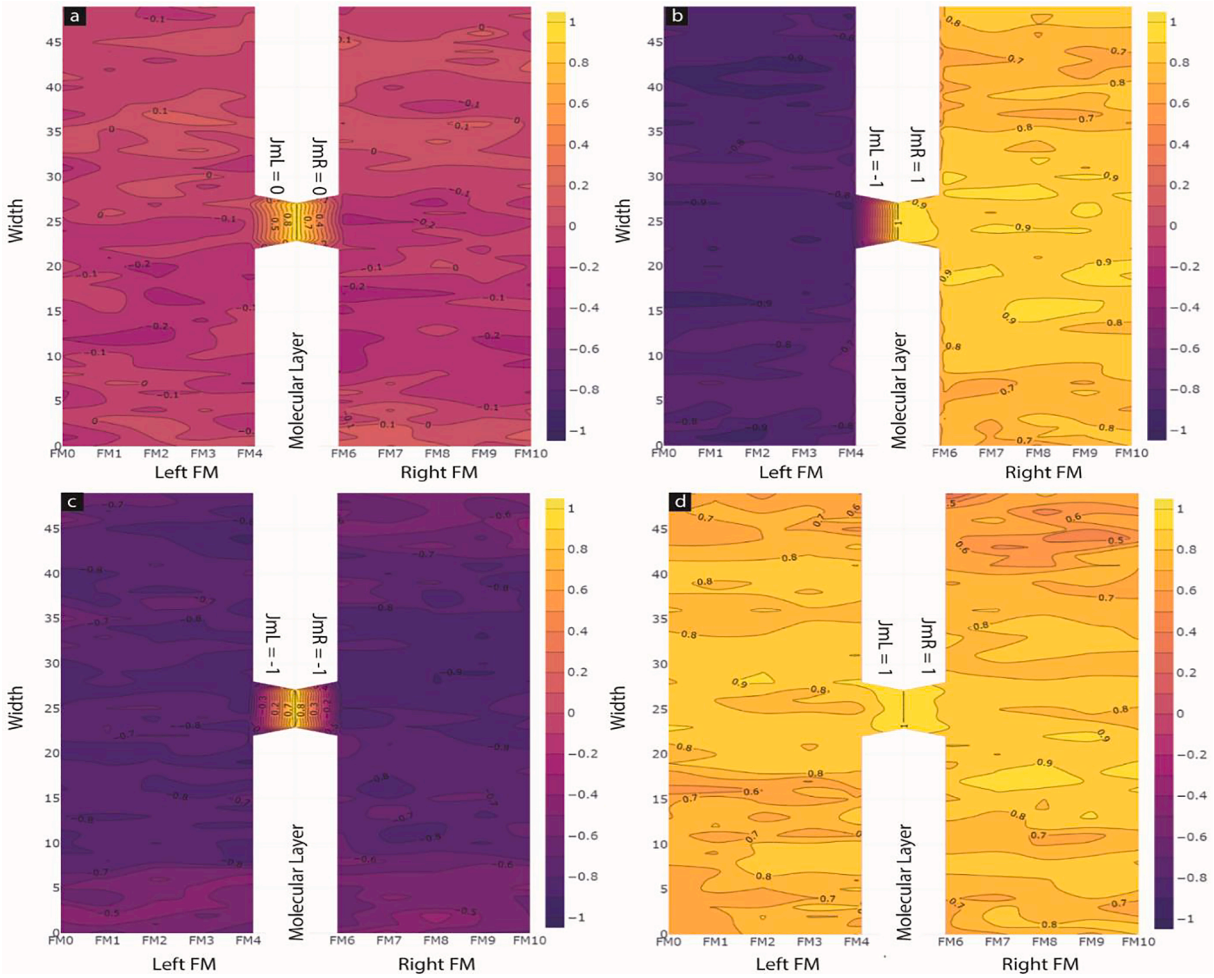

Fig. 4. Autocorrelation contour plots of MTJMSD for all layers of right and left FM electrodes and the magnetic molecule when (a) JmL=JmR=0, (b) *JmL*=−*1*, *JmR*=1, (c) *JmL*=*JmR*= −1 and (d) *JmL*=*JmR*=1.

It is extremely interesting and important to investigate the molecular coupling impact range around FM-molecule interfaces. To characterizing the nature of FM-molecule couplings, the lattice plot showing the spatial distribution of atoms' spins orientation was drawn for the entire MTJMSD (Fig. 3). Simulations were performed for a wide range of exchange coupling strengths and natures. Fig. 3 represents a 3D-lattice plot of the MTJMSD in the direction of the stabilization. The color bar in Fig. 3 varies between 1 to −1 to show the magnitude of molecules and atoms' spin that varies between −1 to 1. A molecule or atom can have a color corresponding to −1 or 1 based on interaction with surrounding entities. As seen in Fig. 3(a–b), when there is no exchange coupling between FM electrodes and molecule ($JmL = 0$, $JmR = 0$), the molecule takes various colors signifying random spin states (Fig. 3c). This causes the molecule to have no control over the FM electrodes' magnetic properties. In our MCS study inter-atomic exchange coupling of both left and right FM electrodes were kept equal ($JL = JR = 1$) which made atoms of each FM electrode to align parallel to each other and resulting in uniform color. In this case two FM electrodes were found to take parallel spin alignment with each other in the equilibrium state attained after 200 Million iterations.

It was hypothesized that increasing magnetic exchange coupling strength between the FM electrodes and the molecule results in correlated states and coherent molecular spin direction. Fig. 3(b) shows an extreme case in which magnetic molecules made antiferromagnetic coupling with the left FM electrode ($JmL = -1$) and ferromagnetic coupling with the right FM electrode ($JmR = 1$). As seen in Fig. 3(b), FM electrodes' spin alignment strongly depends on the exchange couplings with magnetic molecules. In other words, molecules force the FM electrodes' spins to take antiparallel orientation with respect to each other, which leads to magnetic moments cancellation and overall device magnetization close to zero. Interestingly, in a strong coupling regime, the paramagnetic molecule also becomes highly coherent with respect to each other and the FM electrodes (Fig. 3d).

Results discussed in Figs. 2b and 3 provide evidence that 16 molecules forced the two FM electrodes into an antiparallel state. The antiparallel state of ferromagnetic electrodes was only observed when molecules made ferromagnetic exchange coupling with one electrode and antiferromagnetic coupling with another electrode. Fig. 2b shows the time-dependent evolution of MTJMSD magnetic moment under the influence of antiferromagnetic coupling produced by the 16 molecules. The overall magnetic moment of the MTJMSD is the sum of the magnetic moment of left ferromagnet, right ferromagnet, and 16 molecular analogs. An ordered ferromagnet can have a maximum of 1250 magnetic moment because of the 5x5x50 dimension of the Ising Model of each

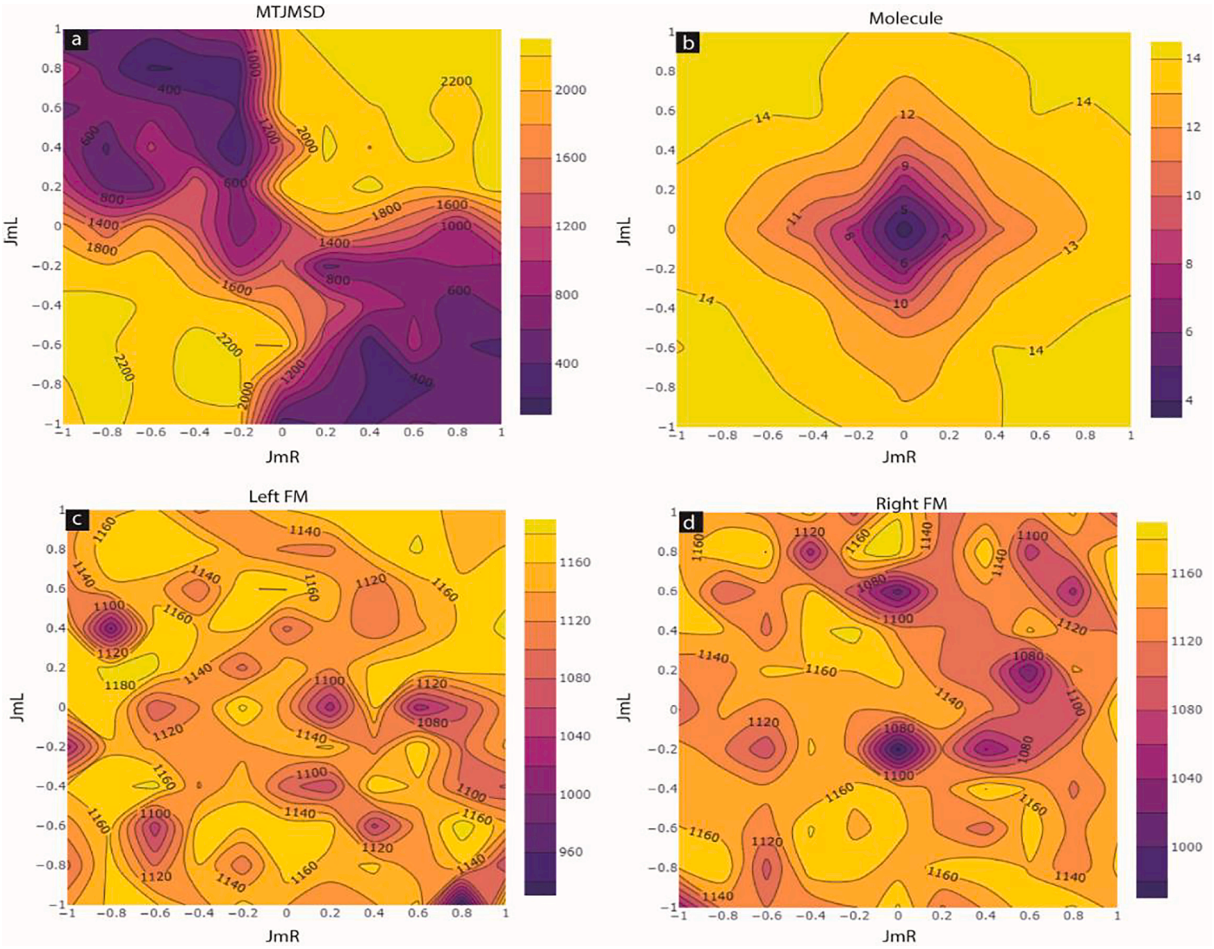

Fig. 5. Contour plot of (a) MTJMSD (b) Molecule (c) left FM electrode and (d) right FM electrode magnetic moment, as a function of FMEs-molecule Heisenberg exchange coupling (JmL and JmR).

electrode. One can hypothesize that if 16 molecules are successful in making two ferromagnetic electrodes antiparallel then the total MTJMSD moment will be settling near 16 or extremely low value because two ferromagnetic electrodes are going to cancel the magnetic moment of each other. MCS simulation data in Fig. 2b directly shows that molecule induced antiferromagnetic exchange coupling forced MTJMSD to settle near 16 or very low magnetic moments that can only occur when two ferromagnetic electrodes are forced by 16 molecules to be antiparallel. Fig. 3b also provides supporting evidence that when 16 molecules are producing the antiferromagnetic coupling between two electrodes the direction of the magnetic moment of the two ferromagnetic electrodes was antiparallel. From these simulations, we learned that only few molecules could influence MTJMSD magnetic properties dramatically. We have also witnessed supporting phenomenon experimentally [15,19] and also showed in the representative magnetic force microscopy image in this paper (Fig. 1e). MFM image was captured on MTJMSD where ~ 10,000 paramagnetic molecules induced antiferromagnetic coupling between microscopic ferromagnetic electrodes over ~ 100 μm range at room temperature. Conforming with the MCS result in Fig. 3b, the MFM study showed that ~ 10,000 molecules could impact MTJMSD's overall magnetic moment and millions of atoms within ferromagnetic electrodes [19]. This result suggests that MTJMSD can be a platform to create highly correlated systems by combining molecular magnetism with ferromagnets.

Simulated 3D Lattice plots shown in Fig. 3 were unable to present the numerical value of the correlation between the molecule and the different regions of FM-electrodes. We hypothesized that computing dot product between molecular spin and the average of atomic spins in each row (along the width) for each FM layer would represent the numerical value of correlation. The equation for computing the correlation is mentioned in Eq. (2).

$$c = (S_m \vec{x} + S_m \vec{y} + S_m \vec{z}).(S_{FM} \vec{x} + S_{FM} \vec{y} + S_{FM} \vec{z}) \quad (2)$$

To complement the previous discussion, we have represented correlation contour plots only for the extreme cases mentioned above. The color bar in Fig. 4 varies between −1 to 1 because the correlation coefficient (c) varies between −1 to 1. Here, −1 demonstrates a strong antiferromagnetic correlation while + 1 shows a strong ferromagnetic correlation between average magnetic moment of molecules and the magnetic moment of individual atoms of the two FM electrodes of the MTJMSD's Ising Model. Fig. 4a demonstrates correlation between molecule and left and right FM electrodes when both Heisenberg couplings are zero ($JmL = JmR = 0$). As was expected from previous results, no correlation exists between FM atomic spin and molecular spin when there is no molecular connection (Fig. 4a). The correlation factor is nearly zero throughout each layer of the two FM electrodes (Fig. 4a).

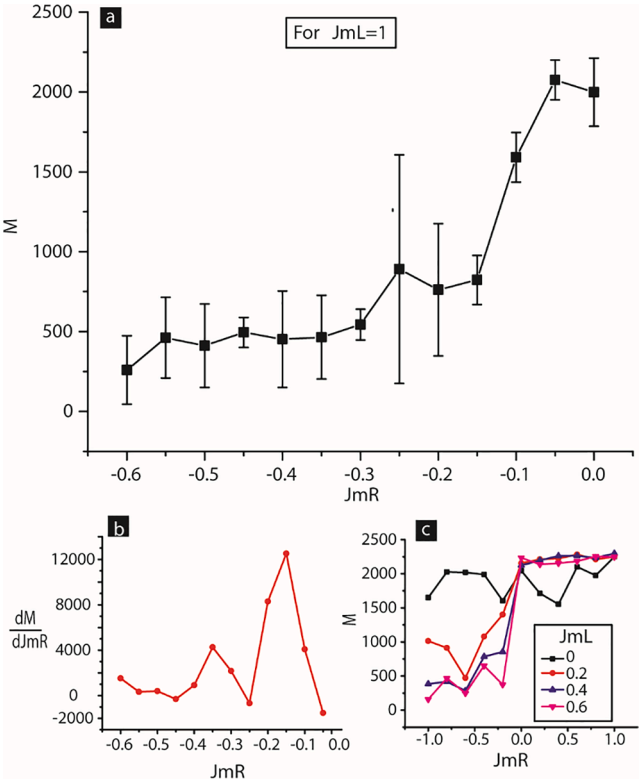

Fig. 6. Two-dimensional illustration of (a) MTJMSD's magnetic moment as a function of *JmR* for *JmL*=1 (b) First derivative of MTJMSD's magnetic moment with respect to *JmR* (c) MTJMSD's magnetic moment as a function of *JmR* for *JmL* values between 0 to 0.6.

However, according to Fig. 4(b–d), a molecule induced strong correlated ferromagnetic alignments when FM-molecule coupling was functional in simulations. It is critical to note that the nature of molecular coupling with FM electrodes defined spatial correlation state on each FM electrodes. For the case of $JmL = -1$ and $JmR = 1$, molecular spin was positively correlated with the right FM electrode and negatively correlated with the left electrode. It is interesting to note that the correlation factor (c) was relatively high around the molecule -FM junction on the right FM electrode (Fig. 4b). Near the FM-molecule junction, there were several regions where c was ~ 0.9. Away from the junction, c was in the 0.7–0.8 range (Fig. 4b). For the $JmL = JmR = -1$ case, when molecular coupling was antiferromagnetic with the left-FM and right-FM, electrode correlation factors (c) was of opposite sign as compared to molecules (Fig. 4c). The magnitude of c was higher close to the molecule-FM interface and started waning away from the junction area. Strongly correlated regions appeared in randomly shaped regions (Fig. 4c). For the $JmL = JmR = 1$ case, when molecular coupling was ferromagnetic in nature with both FM electrodes, c possessed the same sign for the molecule and FM electrodes (Fig. 4d). The magnitude of c was higher close to the FM-molecule interfacial region and was slightly lower away from the junction (Fig. 4d).

For gaining a detailed picture of MTJMSD magnetic behavior, contour plots of MTJMSD's magnetic moments were drawn for a wide range of *JmR* and *JmL* values. In this paper, we have discussed 121 cases of molecule-FM electrode couplings in Fig. 5. Also, we systematically weaken the FM-molecule coupling strength to investigate the resultant MTJMSD properties in Fig. 6. Results discussed in Figs. 5 and 6 provide the impact of molecular exchange couplings over a wide range in addition to extreme cases discussed in Figs. 2–4. Overall device magnetization is determined by adding molecule, left FM, and right FM's magnetic moments. The color bar in Fig. 5 corresponds to the range of magnetic moment observed for MTJMSD (Fig. 5a), molecules (Fig. 5b), left and right ferromagnet electrodes (Fig. 5c–d). Due to the device configuration used in our MCS study, each electrode can gain up to 1250 magnetic moment magnitude and molecules can attain up to 16 magnetic moment magnitude. Thus, total MTJMSD magnetization varies between zero to 2516 magnitude. *JmL* and *JmR* were varied over −1 to 1 range to encompass all the possible combinations. It is noteworthy that the Curie temperature of FM electrodes is one because of $J_L = J_R = 1$. Hence, $|JmL|=|JmR|=1$ signifies that the molecule induced exchange coupling is comparable with the interatomic bonding. According to Fig. 5(a), maximum MTJMSD magnetization intensity occurs when two FM electrodes make ferromagnetic coupling through magnetic molecules. Similarly, high MTJMSD magnitude was observed when the molecule produced antiferromagnetic coupling with the two FM electrodes. Interestingly, MTJMSD settled into a low magnetic moment state in the event when the sign or nature of *JmL* and *JmR* were opposite to each other. It appears that high to low magnetic moment transition was possible when $|JmL|$ and $|JmR|$ was around 0.1. Thus, the transition point is observed around 10% of Curie temperature. The contour plot of molecules' magnetic moment changed significantly as a function of molecular coupling strength. Molecules' magnetic moment was in general high due to correlated state with two FM electrodes. With *JmL* and *JmR* settling to zero, the molecular magnetic moment settled close to zero (Fig. 5b). The magnetic moment of the two FM electrodes remained between the 1000 to 1200 range for every molecular magnitude and type (Fig. 5c–d).

To estimate the critical values of molecular coupling when an MTJMSD transcends from high to low magnetization, we drew the two-dimensional plot of the magnetic moment for various molecule-FM electrodes' exchange coupling. Keeping $JmL = 1$, the *JmR* was varied over the 0 to −0.6 range (Fig. 6a). The first derivative of the curve mentioned in (Fig. 6b) provided the critical *JmR*. Fig. 6b shows that transition started to happen at around 20% of the Curie temperature. Fig. 5c illustrates MTJMSD's magnetic moment for $JmL = 0$ to 0.6, as a function of different *JmR* values. According to the graph, when there is no coupling with one of the electrodes ($JmL = 0$), no transition can be expected. In other words, the lack of interaction between electrodes and the molecule results in no correlation between FM electrodes. However, the role of magnetic coupling via molecules can be observed in all other cases ($0.2 < JmR$ less than 0.6) shown in Fig. 6c. As the results imply, the transition point is consistently around 0.1 ± 0.05. This result provides an important insight that when molecule-induced antiferromagnetic coupling is ~ 0.15 a large area of FM electrode can be impacted.

To investigate the switching attributes, we calculated the spatial magnetic susceptibility in different sections of MTJMSD (Fig. 7). Magnetic susceptibility was calculated by considering the group of atoms present along the width of FM electrodes. In the event when $JmL = JmR = 0$, the molecule section exhibited nearly seven times more magnetic susceptibility as compared to the FM electrodes (Fig. 7a). This situation is possible when molecule-FM bonding is negligible. In such a case, molecules can selectively respond to the magnetic field. For the case of $JmL = 1$ *and* $JmR = -1$, the molecular region magnetic susceptibility is similar to that of FM electrodes. In this case, molecule and FM electrodes are expected to respond to the external magnetic field, and selective switching of the magnetic moment of molecule and FM electrodes may

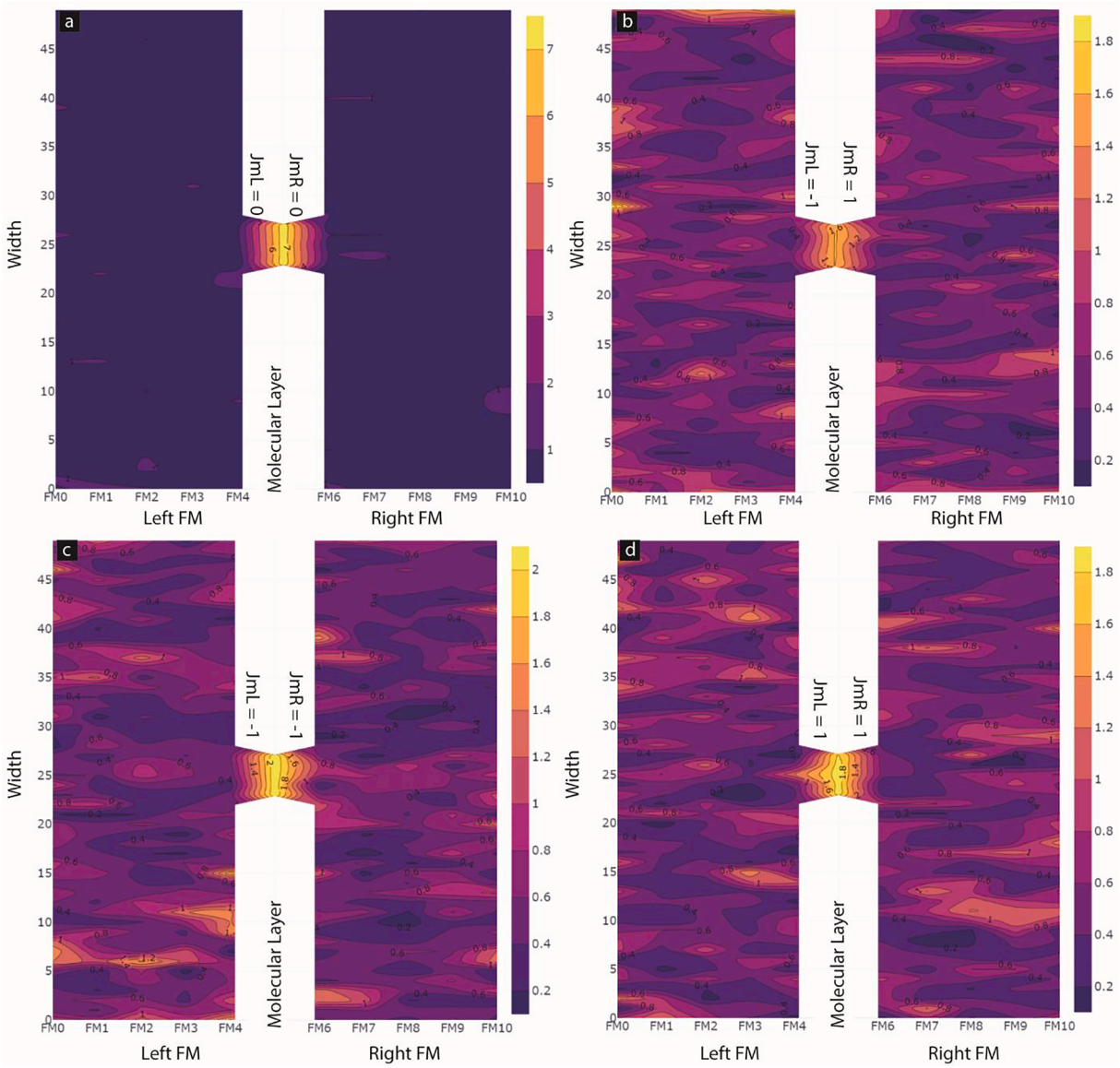

Fig. 7. Magnetic Susceptibility contour plots of MTJMSD for all layers of right and left FM electrodes and the magnetic molecule when (a) *JmL*=*JmR*=0, (b) *JmL*=*−1, JmR*=1, (c) *JmL*=*JmR*= −1 and (d) *JmL*=*JmR*=1.

be extremely challenging (Fig. 7b). Interestingly, for the situation when $JmL = JmR = -1$, the magnetic susceptibility of the molecule is 2 to 10 times higher than that of FM electrodes (Fig. 7c). However, in this situation, FM electrodes' exhibit non-uniform distribution of magnetic susceptibility. The non-uniform distribution is expected to be caused by the molecule induced correlation shown in Fig. 4. Similarly, for the $JmL = JmR = 1$, the magnetic susceptibility of the molecular region was 2–10 times higher than the FM electrodes. Also, FM electrodes possessed non-uniform magnetic susceptibility distribution (Fig. 7d). We conclude that to attain a switching phenomenon where the molecules' magnetic moment can be switched independently, molecular coupling either has to be negligible or of the same sign (ferromagnetic or antiferromagnetic) with two electrodes. These characteristics motivate us to study MTJMSD behavior in the presence of a magnetic field in our future study.

4. Conclusion

Monte Carlo simulation was used to investigate the effect of variation of coupling strengths and nature between the magnetic molecules and ferromagnetic electrodes on magnetic tunnel junction (MTJ)-based molecular spintronic devices (MTJMSD). When two electrodes have similar and strong magnetization (both ferromagnetic or both antiferromagnetic), device magnetization is maximum, and its magnitude remains between 2000 and 2500. Decreasing total device magnetization can be a sign of molecule-induced strong antiferromagnetic coupling. Under the impact of molecule-induced antiferromagnetic coupling effect, two FM electrodes tend to align antiparallel with respect to each other. Our results showed that in the cases when molecular coupling strength was more than ∼ 20% of the ferromagnetic electrode's Curie temperature, 16 molecules could influence the magnetic properties of

2,500 atoms above room temperature. This theoretical study is directly in agreement with the experimental observation of ~ 10,000 molecular coupling controlling the microscopic MTJ testbed's physical properties. This paper also showed that the molecule-induced coupling effect was stronger near junction areas. Our magnetic susceptibility study suggested that magnetic field-induced switching is highly likely for the extremely weak molecular coupling strengths or when the sign of molecular coupling with two ferromagnetic electrodes is the same. In a future study, we aim to study cross-junction shaped MTJMSD of large dimensions by varying the thermal energy and magnetic field.

Declaration of Competing Interest

The authors declare that they have no known competing financial interests or personal relationships that could have appeared to influence the work reported in this paper.

Acknowledgements

We gratefully acknowledge the funding support from National Science Foundation-CREST Award (Contract # HRD- 1914751), and Department of Energy/National Nuclear Security Agency (DE-FOA-0003945). We also acknowledge the support of The Center for Nanoscale Science and Technology (CNST) at the National Institute of Standards and Technology (NIST). All the views in this paper are of the authors and do not represent any organization, institute, or funding agency.

References

[1] E. Coronado, A.J. Epsetin, Molecular spintronics and quantum computing, J. Mater. Chem. 19 (12) (2009) 1670–1671.
[2] R. Sessoli, Molecular nanomagnetism in Florence: advancements and perspectives, Inorg. Chim. Acta 361 (12-13) (2008) 3356–3364.
[3] L. Bogani, W. Wernsdorfer, Molecular spintronics using single-molecule magnets, Nat. Mater. 7 (3) (2008) 179–186.
[4] S. Sanvito, Injecting and controlling spins in organic materials, J. Mater. Chem. 17 (42) (2007) 4455–4459.
[5] S. Sanvito, Molecular spintronics the rise of spinterface science, Nat. Phys. 6 (8) (2010) 562–564.
[6] S. Sanvito, Molecular spintronics, Chem. Soc. Rev. 40 (6) (2011) 3336, https://doi.org/10.1039/c1cs15047b.
[7] S. Sanvito, A.R. Rocha, Molecular-spintronics: the art of driving spin through molecules, J. Comp. Theor. Nanosci. 3 (5) (2006) 624–642.
[8] S.M. Yakout, Spintronics: future technology for new data storage and communication devices, J. Supercond. Novel Magn. 33 (9) (2020) 2557–2580.
[9] N. Prokopuk, K.-A. Son, Alligator clips to molecular dimensions, J. Phys. Condens. Matter 20 (37) (2008) 374116, https://doi.org/10.1088/0953-8984/20/37/374116.
[10] Y. Selzer, L. Cai, M.A. Cabassi, Y. Yao, J.M. Tour, T.S. Mayer, D.L. Allara, Effect of local environment on molecular conduction: isolated molecule versus self-assembled monolayer, Nano Lett. 5 (1) (2005) 61–65.
[11] A.N. Pasupathy, R.C. Bialczak, J. Martinek, J.E. Grose, L.A.K. Donev, P.L. McEuen, D.C. Ralph, The Kondo effect in the presence of ferromagnetism, Science 306 (5693) (2004) 86–89.
[12] J.R. Petta, S.K. Slater, D.C. Ralph, Spin-dependent transport in molecular tunnel junctions, Phys. Rev. Lett. 93 (13) (2004), https://doi.org/10.1103/PhysRevLett.93.136601.
[13] P. Tyagi, E. Friebe, C. Baker, Advantages of prefabricated tunnel junction based molecular spintronics devices, NANO 10 (04) (2015) 1530002, https://doi.org/10.1142/S1793292015300029.
[14] P. Tyagi, Multilayer edge molecular electronics devices: a review, J. Mater. Chem. 21 (13) (2011) 4733–4742.
[15] P. Tyagi, C. Baker, C. D'Angelo, Paramagnetic molecule induced strong antiferromagnetic exchange coupling on a magnetic tunnel junction based molecular spintronics device, Nanotechnology 26 (30) (2015) 305602, https://doi.org/10.1088/0957-4484/26/30/305602.
[16] Y.M. Leeor Kronik, Understanding the metal–molecule interface from first principles, in: N.U. Norbert Koch, T.S. Andrew, Wee (Eds.), The Molecule–Metal Interface, 2013, pp. 51–89.
[17] P. Tyagi, C. Riso, E. Friebe, Magnetic tunnel junction based molecular spintronics devices exhibiting current suppression at room temperature, Organ. Electron. 64 (2019) 188–194.
[18] P. Tyagi, C. Riso, Molecular spintronics devices exhibiting properties of a solar cell, Nanotechnology 30 (49) (2019) 495401, https://doi.org/10.1088/1361-6528/ab3ab0.
[19] P. Tyagi, C. Riso, Magnetic force microscopy revealing long range molecule impact on magnetic tunnel junction based molecular spintronics devices, Organ. Electron. 75 (2019) 105421, https://doi.org/10.1016/j.orgel.2019.105421.
[20] P. Tyagi, E. Friebe, Large resistance change on magnetic tunnel junction based molecular spintronics devices, J. Mag. Mag. Mat. 453 (2018) 186–192.
[21] A. Grizzle, C. D'Angelo, P. Tyagi, Monte Carlo simulation to study the effect of molecular spin state on the spatio-temporal evolution of equilibrium magnetic properties of magnetic tunnel junction based molecular spintronics devices, AIP Adv. 11 (1) (2021) 015340, https://doi.org/10.1063/9.0000228.
[22] H. Brown, A. Grizzle, C. D'Angelo, B.R. Dahal, P. Tyagi, Impact of direct exchange coupling via the insulator on the magnetic tunnel junction based molecular spintronics devices with competing molecule induced inter-electrode coupling, AIP Adv. 11 (1) (2021) 015228, https://doi.org/10.1063/9.0000225.
[23] C. Kittel, Introduction to Solid State Physics, 7th ed., John Wiley & Sons, Inc, 1996.